

Spectrum Sensing For Cognitive Radios Through Differential Entropy

Sanjeev Gurugopinath¹, R. Muralishankar^{2,*} and H. N. Shankar³
Emails: sanjeevg@pes.edu, {muralishankar,hnshankar}@cmrit.ac.in

¹Department of Electronics and Communication Engineering, PES University, Bengaluru 560085.

²Department of Electronics and Communication Engineering, CMR Institute of Technology, Bengaluru 560037.

³Department of Electrical and Electronics Engineering, CMR Institute of Technology, Bengaluru 560037.

Abstract

In this work, we present a novel Goodness-of-Fit Test driven by differential entropy for spectrum sensing in cognitive radios, under three different noise models – Gaussian, Laplacian and mixture of Gaussians. We analyze the proposed detector under Gaussian noise which models the worst-case. We then analyze by considering the Laplacian noise process which has tails heavier than that of the Gaussian. We generalize the analysis considering the noise to be a mixture of Gaussians, which is often the case with noise and interference in communication systems. We analyze the performance under each of these cases for a large class of practically relevant fading channel models and primary signal models, with emphasis on low Signal-to-Noise ratio regimes. Towards this end, we derive closed form expressions for the distribution of the test statistic under the null hypothesis and the detection threshold that satisfies a constraint on the probability of false-alarm. Through Monte Carlo simulations, we demonstrate that our detection strategy outperforms an existing spectrum sensing technique based on order statistics.

Received on 15 August, 2015; accepted on 4 December, 2015; published on 05 April, 2016

Keywords: Spectrum sensing, goodness-of-fit, differential entropy, maximum entropy principle, non-Gaussian noise.

Copyright © 2016 S. Gurugopinath *et al.*, licensed to EAI. This is an open access article distributed under the terms of the Creative Commons Attribution license (<http://creativecommons.org/licenses/by/3.0/>), which permits unlimited use, distribution and reproduction in any medium so long as the original work is properly cited.

doi:10.4108/eai.5-4-2016.151147

1. Introduction

Goodness-of-Fit Tests (GoFT) for Spectrum Sensing (SS) has received considerable attention in the recent past [2–6]. This approach may be gainfully employed in Cognitive Radio (CR) when a proper knowledge of the primary signal and the fading models is far from complete. In its general form, the GoFT for SS compares a decision statistic to a threshold and rejects the null-hypothesis when the statistic exceeds the threshold. The detection threshold is chosen so as to satisfy a constraint on the probability of false-alarm.

The authors in [2] present a GoFT based on the Anderson-Darling statistic (which we term here as the Anderson-Darling statistic based Detector (ADD)). This is shown to outperform the well-known radiometer or Energy Detector (ED) under low SNR regime with

Rayleigh fading and constant primary signal. Later, it is shown that a combination of the Student's-t Test and the ADD, called the Blind Detector (BD) [3], is robust to noise variance uncertainty. The major infirmities of these works are as follows: (i) The underlying Anderson-Darling statistic is known to perform well only against another Gaussian with a shift in mean. ADD does not perform well in many other relevant SS contexts as, for example, when the primary signal follows other signal models [7]. (ii) The ADD is useful only where the observations under \mathcal{H}_0 are i.i.d. (iii) ADD is effective only with small number of observations. Thus, the utility of ADD and BD in SS is diminished.

In [4], the authors propose an Order Statistic based Detector (OSD) and show that it improves upon ADD under conditions discussed in the foregoing. Here, the performance of OSD detector is studied only for a constant primary model. Further, the threshold is set empirically. A Higher Order statistics based Detector [6]

*Corresponding author. Email: muralishankar@cmrit.ac.in
This work has appeared in part in [1].

is shown to provide good performance under low SNR. Recently, a zero-crossings based GoFT [5] is shown to be robust to uncertainties of the noise model and the parameters; its computational complexity matches that of the GoFT based on ED.

In this work, we propose a novel GoFT based on an estimate of the differential entropy in the received observations. We bring out the many advantages of this technique: (i) relative ease in computing the detection threshold; (ii) relaxation of the restriction of a constant primary signal; and (iii) enhanced performance relative to OSD in several situations which are practically realistic. Additionally, we study the performance of the detector for the Laplacian noise model and a bimodal, two parameter mixed Gaussian noise model. In fact, the mixed Gaussian noise is used, inter alia, to model a combination of Gaussian and Middleton's class A noise components [5] and co-channel interference (CCI) [8]. Further, we obtain a closed-form expression for the optimal detection thresholds for spectrum sensing, considering Gaussian and Laplacian noise models and the near-optimal detection threshold for the mixed Gaussian.

The system model is described in § 2. Differential entropy estimate based detection is introduced and analyzed in § 3. In particular, the cases where the noise process is purely Gaussian, is Laplacian and follows a bimodal Gaussian are studied in § 3.1-3.3 successively. Simulation results are presented and discussed in § 4. Concluding remarks comprise § 5.

2. System Model

Consider a CR node collecting M observations from a primary transmitter operating in a particular frequency band. Based thereon, it decides whether the band is occupied or vacant. The GoFT based SS problem is essentially a detection problem which rejects the noise-only hypothesis given by

$$\mathcal{H}_0 : Y_i \sim f_{\mathbb{N}}, \quad i \in \mathcal{M} \triangleq \{1, \dots, M\},$$

with the probability of false alarm given by

$$p_f \triangleq \mathcal{P}\{\text{reject } \mathcal{H}_0 | \mathcal{H}_0\} \leq \alpha_f,$$

where $\alpha_f \in (0, 1)$ is a fixed constant. The noise distribution $f_{\mathbb{N}}$ for SS can be modeled by various distributions [5]. In this paper, we consider the following: Gaussian, Laplacian and mixture of Gaussians. First, for the sake of simplicity and to study the baseline, we consider the Gaussian, which is adopted in many spectrum sensing approaches. Second, we look at the Laplacian noise having tail heavier than Gaussian. Finally, we take up the bimodal Gaussian distribution, known to be useful in some applications in communication domains [8].

We develop a detector based on the following assumptions:

- (a) Noise variance is known perfectly;
- (b) The statistics of the primary signal model and the fading channel between the primary transmitter and CR node can be arbitrary.

2.1. Effect of Noise Variance Uncertainty

In practice, the estimate of the noise variance can deviate significantly from its true value, leading to a poor performance of the detector, especially under low SNR regime [3]. Note that our detector can be made robust to the noise variance uncertainty by considering the technique followed in [3]. The detector proposed in this work can be combined with the Student's t-test, similar to the combination of the Anderson-Darling statistic based test with the Student's t-test, discussed in [3]. A detailed study of the performance of the combined detector is currently work in progress.

We present the Order Statistic-based Detector (OSD) [4], known to be the best GoFT detector for testing $f_{\mathbb{N}}$ against a mean-change model, and its implementation in the following subsection.

2.2. The Order Statistic-Based Detector (OSD) [4]

We outline the key steps involved in the construction of the OSD.

1. Let $F_{\mathbb{N}}$ be the Cumulative Distribution Function (CDF) of the noise process. Obtain a transformation on the received observations, Y_i , as

$$z_i = F_{\mathbb{N}}(Y_i), \quad i \in \mathcal{M}.$$

2. Sort the variables z_i as

$$z_{(1)} \leq z_{(2)} \leq \dots \leq z_{(M)}.$$

3. Obtain the beta transformation on $z_{(i)}$ as

$$\rho_i \triangleq \sum_{j=i}^M \frac{M!}{(M-j)!j!} z_{(i)}^j [1 - z_{(i)}]^{M-j}, \quad i \in \mathcal{M}$$

and then, sort as

$$\rho_{(1)} \leq \rho_{(2)} \leq \dots \leq \rho_{(M)}.$$

4. The OSD is devised thus:

$$\sum_{i=1}^M \left| \rho_{(i)} - \frac{i}{(M+1)^2} \right| \underset{\sim \mathcal{H}_0}{\overset{\sim \mathcal{H}_0}{\geq}} \tau_{\text{OS}}.$$

Here, for some fixed false-alarm $\alpha_f \in (0, 1)$, the optimal threshold, τ_{OS} , is given by [4]

$$\begin{aligned} \tau_{\text{OS}} = & 2.599 + 0.8228M - 30.79\alpha_f + 73.75\alpha_f^2 \\ & - 49.08\alpha_f^3 - 0.6466\alpha_f M. \end{aligned}$$

The proposed differential entropy estimate based GoFT is discussed in the following section.

3. Differential Entropy Estimate-based GoFT

The differential entropy, denoted by $h(X)$, for a continuous random variable X is defined as [9]

$$h(X) \triangleq - \int_{-\infty}^{\infty} f_X(x) \log(f_X(x)) dx$$

where $f_X(\cdot)$ is the probability density function of X .

In this technique, we estimate the differential entropy in the observations and use it as a test statistic to carry out spectrum sensing. We derive the distribution of the statistic and the value of the optimal detection threshold next, which depend on the noise statistics.

3.1. Detection Under Gaussian Noise

Let $f_{\mathbb{N}} \sim \mathcal{N}(0, \sigma_n^2)$, where $\mathcal{N}(\mu, \sigma^2)$ represents the Gaussian distribution with mean μ and variance σ^2 . The detection strategy proposed in this work exploits the fact that among all continuous distributions with finite mean and variance, and with support $(-\infty, \infty)$, the Gaussian yields maximum differential entropy. For this detector, the entropy when $Y_i \sim f_{\mathbb{N}}, i \in \mathcal{M}$ (i.e., for observations under \mathcal{H}_0), is less than the entropy if the primary is present, i.e., $Y_i \approx f_{\mathbb{N}}$. It is known that under \mathcal{H}_0 , i.e., when $Y_i \sim \mathcal{N}(0, \sigma_n^2)$ [9],

$$h(Y|\mathcal{H}_0) = \frac{1}{2} \log(2\pi e \sigma_n^2).$$

Now, the Differential Entropy estimate-based Detector (DED) is constructed for a given set of observations with sample mean and variance

$$\widehat{Y} \triangleq \frac{1}{M} \sum_{i=1}^M Y_i \quad \text{and} \quad \frac{1}{M-1} \sum_{i=1}^M (Y_i - \widehat{Y})^2$$

respectively. Then,

$$\widehat{h}(Y) \triangleq \frac{1}{2} \log \left\{ \frac{2\pi e}{M-1} \sum_{i=1}^M (Y_i - \widehat{Y})^2 \right\}$$

represents the maximum likelihood estimate of differential entropy in the observations. The test is of the form

$$\widehat{h}(Y) \underset{\sim \mathcal{H}_0}{\overset{\sim \mathcal{H}_0}{\gtrless}} \tau_G,$$

where τ_G is set such that a constraint on the probability of false-alarm, α_f , is satisfied. See Appendix A for a procedure to find the optimal τ_G given α_f .

3.2. Detection Under Laplacian Noise

It is known that for the Laplacian distribution, $\mathcal{L}(\lambda)$, with parameter λ , the differential entropy is given by

$$h(Y|\mathcal{H}_0) = \log_2(2e\lambda),$$

where $\lambda \triangleq \sqrt{\sigma_n^2/2}$. An unbiased estimate of λ is given by

$$\widehat{\lambda} = \frac{1}{M} \sum_{i=1}^M |Y_i - \widehat{Y}|,$$

where \widehat{Y} denotes the estimate of the $\frac{1}{2}$ -median. Therefore, an estimate of $h(\cdot)$ is obtained as

$$\widehat{h}(Y) \triangleq \log_2 \left(\frac{2e}{M} \sum_{i=1}^M |Y_i - \widehat{Y}| \right),$$

and hence, the test is

$$\widehat{h}(Y) \underset{\sim \mathcal{H}_0}{\overset{\sim \mathcal{H}_0}{\gtrless}} \tau_L.$$

Here, τ_L is set such that a constraint on the probability of false-alarm, α_f , is satisfied. See Appendix B for computing τ_L given α_f .

3.3. Detection Under Mixed Gaussian Model

The mixed Gaussian noise model is considered in a variety of signal processing applications for communications. For instance, it is used to model a combination of thermal noise and man-made clutter noise [5], and the Co-Channel Interference (CCI) [8]. Some non-Gaussian noise processes can also be modeled as mixtures of Gaussians [10]. The PDF of the mixture Gaussian noise is [11]

$$f_{\mathbb{N}}(x) = \frac{1}{\sqrt{2\pi\sigma_n^2}} e^{-(x^2+\mu^2)/(2\sigma_n^2)} \cosh\left(\frac{\mu x}{\sigma_n^2}\right). \quad (1)$$

In general, the differential entropy of this two-component mixture-Gaussian model is expressed implicitly as

$$h(Y|\mathcal{H}_0) = \frac{1}{2} \log(2\pi e \sigma_n^2) + \left(\frac{\mu}{\sigma_n}\right)^2 - \mathcal{I}.$$

\mathcal{I} for different μ and σ_n are tabulated [11]. Also, expressions for tight upper and lower bounds on the entropy are reported [11]. Thus, under \mathcal{H}_0 ,

$$\begin{aligned} h_{UB}(Y|\mathcal{H}_0) &\leq \frac{1}{2} \log(2\pi e \sigma_n) + \left(\frac{\mu}{\sigma_n}\right)^2 \left\{ 1 - \operatorname{erf}\left(\frac{\mu}{\sqrt{2\sigma_n^2}}\right) \right\} \\ &\quad - \sqrt{\frac{2\mu^2}{\pi\sigma_n^2}} e^{-\mu^2/(2\sigma_n^2)} + \log 2, \\ h_{LB}(Y|\mathcal{H}_0) &\geq \frac{1}{2} \log(2\pi e \sigma_n) + \left(\frac{\mu}{\sigma_n}\right)^2 \left\{ 1 - \operatorname{erf}\left(\frac{\mu}{\sqrt{2\sigma_n^2}}\right) \right\} \\ &\quad - \sqrt{\frac{2\mu^2}{\pi\sigma_n^2}} e^{-\mu^2/(2\sigma_n^2)}. \end{aligned}$$

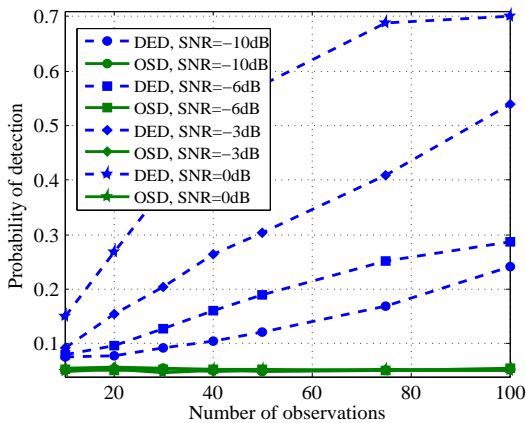


Figure 1. Probability of detection: DED and OSD for different M and SNRs | Gaussian primary signal | Nakagami- m fading: Shape parameter = 1, Scale parameter = 0.5.

We choose the upper bound as a test statistic for SS against the PDF of (1). Based on the estimates, the test is

$$\widehat{h}_{UB}(Y) \underset{\sim \mathcal{H}_0}{\overset{\sim \mathcal{H}_1}{\geq}} \tau_{MG}.$$

Note that the above test is pessimistic, i.e., it follows the worst-case design. Obtaining the exact PDF of the test statistic in this case is difficult. Therefore, we estimate the PDF of the test statistic and set the threshold through Monte Carlo simulations. Further, we provide the asymptotically optimal threshold for this setting (vide Appendix C).

4. Simulation Results

We evaluate the SS performance of DED and OSD through extensive simulations under various primary signal models, noise models and fading. The primary signal models chosen are constant and Gaussian, while the noise models are Gaussian, Laplacian and mixture of Gaussians. We employ fading models such as Nakagami- m , Weibull and Rayleigh. Nakagami- m (and as its special case, Rayleigh) fading is favored for several indoor wireless communication without line of sight [12]. For some applications in communication with frequency in excess of 900MHz, Weibull fading is found to be a good fit [12]. We set the false-alarm, α_f , to 0.05 and vary the SNR from -10dB to 0dB.

The performance of DED and OSD under the Gaussian noise (vide Fig. 1) shows the probability of detection (p_d) using DED and OSD for M observations and for different values of SNR under Nakagami- m fading with shape and scale parameters 1 and 0.5 respectively. These fading parameters are chosen arbitrarily. The primary signal is taken to be Gaussian [5]. Such an assumption is practically relevant in CR context owing to the errors due to synchronization

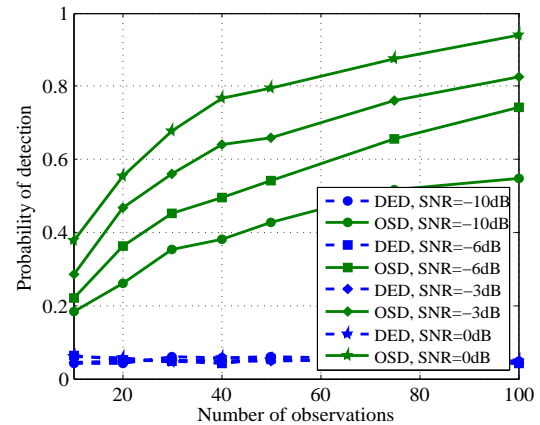


Figure 2. Probability of detection: DED and OSD vs. M for different SNRs | Constant primary signal | Nakagami- m fading: Shape parameter = 1, Scale parameter = 0.5.

and timing offsets. As can be seen, DED outperforms OSD. The performance of OSD is non-trivial, i.e., it operates on the chance line in the receiver operating characteristics.

Fig. 2 presents p_d when the primary signal is constant. We observe that the OSD fares better than DED. Under a constant primary, such performance benefits of the OSD have been observed earlier [4]. A point to note is that the constant primary assumption is largely of theoretical interest as it is highly constrained [13]. Further, the deteriorated performance of DED is due to invariance of entropy to scaling [9].

Fig. 3 presents p_d under Weibull fading, with shape and scale parameters 1 and 2 respectively. The fading parameters are set arbitrarily. The primary signal is Gaussian. Evidently, DED is better than OSD across all M and SNRs. For a constant primary signal with the Weibull fading and with the same parameters as before, OSD is seen to outperform DED (vide Fig. 4). When the primary signal is not constant, the pattern shows DED better than OSD. Similar conclusions can be drawn from Fig. 5 which presents p_d for varying SNRs under Rayleigh fading with parameter 1 and Gaussian primary signal.

Next, we evaluate DED and OSD under Laplacian noise model with the primary being Gaussian and Rayleigh fading. Fig. 6 and Fig. 7 show p_d vs. M and p_d vs. average primary SNR respectively. The noise variance is assumed to be unity. Yet again, OSD proves to perform only trivially in both cases due to primary variation. However, the performance of DED improves significantly with an increase in M and SNR. Additionally, comparing Fig. 5 and Fig. 6, we can see that the p_d with Gaussian noise is higher than p_d with Laplacian noise. This effect is due to the heavy-tailed nature of the Laplacian distribution, i.e., owing to elevated tail probabilities, the detection threshold that

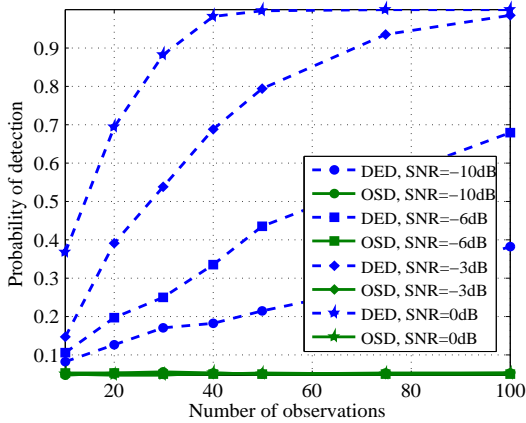


Figure 3. Probability of detection: DED and OSD vs. M for different SNRs | Gaussian primary signal | Weibull fading; Shape parameter = 1, Scale parameter = 2.

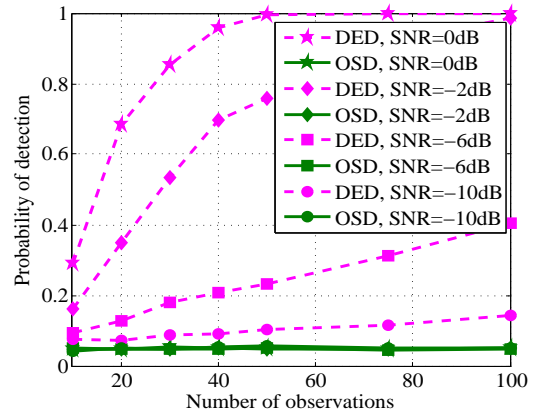


Figure 6. Probability of detection: DED and OSD vs. M for different primary SNRs | Rayleigh fading | Laplacian noise | Gaussian primary signal.

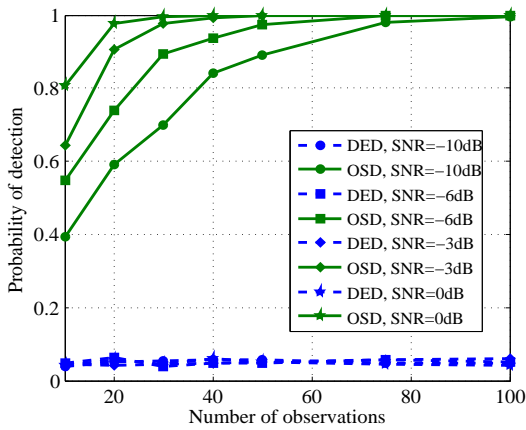


Figure 4. Probability of detection: DED and OSD vs. M for different SNRs | Constant primary signal | Weibull fading; Shape parameter = 1, Scale parameter = 2.

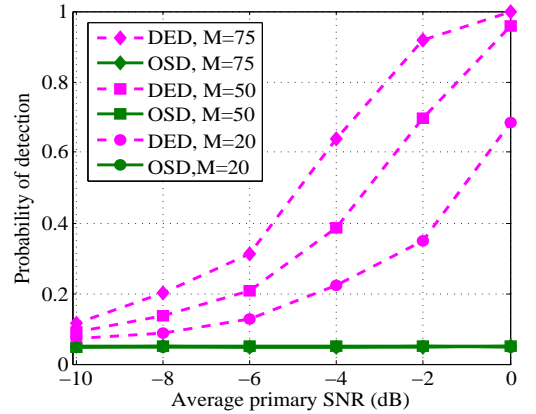


Figure 7. Probability of detection: DED and OSD vs. M for different SNRs | Rayleigh fading | Laplacian noise | Gaussian primary signal.

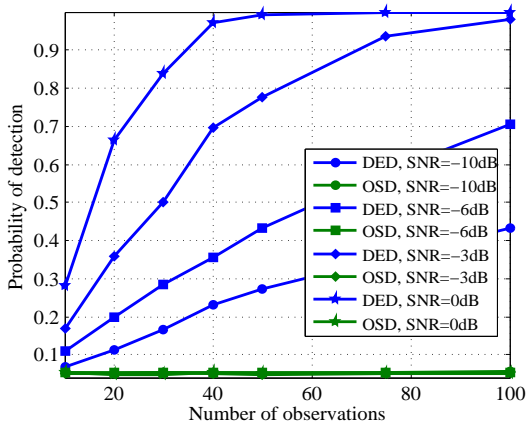


Figure 5. Probability of detection: DED and OSD vs. M for different SNRs | Gaussian primary signal | Rayleigh fading; Parameter = 1.

satisfies the given false-alarm increases, which in turn pulls down p_d .

We now move from a unimodal probability density assumption for the noise to a bimodal Gaussian (mixture of two Gaussians) [8] to evaluate DED and OSD. We present p_d with DED and OSD taking the primary signal as Gaussian and the fading as Rayleigh. Fig. 8 and Fig. 9 show p_d vs. average primary SNR and p_d vs. M respectively. We set $\mu = 2$ and the mixing parameter as 0.5. We note that the the performance of OSD is trivial, whereas DED outperforms OSD. As expected, the performance of DED improves with increase in SNR and M . The shortcomings of OSD lends credence to the proposition that its usefulness is restricted to the case of Gaussian noise and constant primary signal.

We present the utility of Gaussian mixture assumption for noise, by comparing the performance of DED

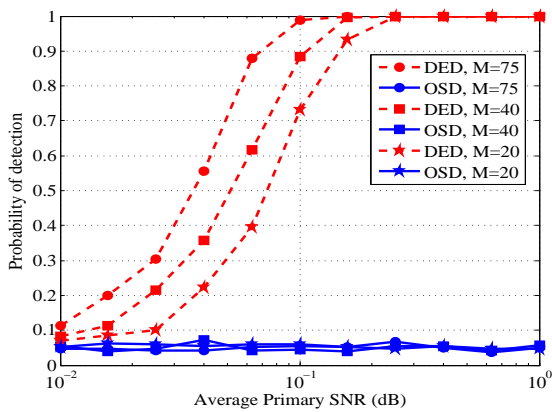


Figure 8. Probability of detection: DED and OSD vs. average primary SNR for different M | Rayleigh fading | Mixture Gaussian noises | Gaussian primary signal.

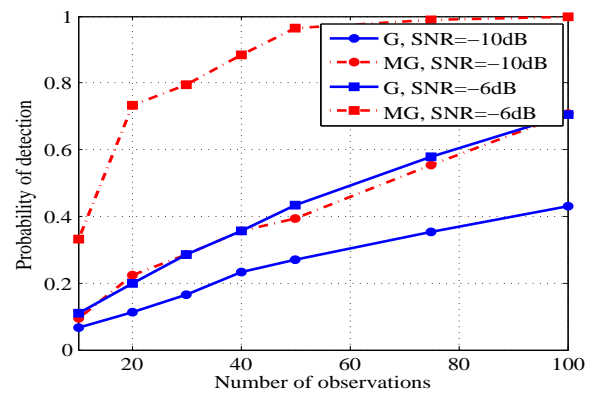


Figure 10. Probability of detection: DED and OSD vs. M for different primary SNRs | Rayleigh fading | Gaussian and mixture Gaussian noises | Gaussian primary signal.

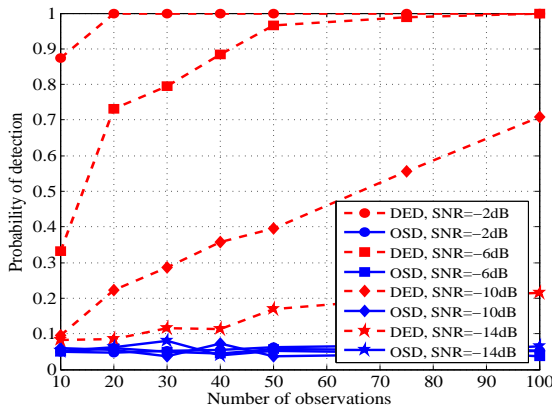


Figure 9. Probability of detection: DED and OSD vs. M for different average primary SNRs | Rayleigh fading | Mixture Gaussian noises | Gaussian primary signal.

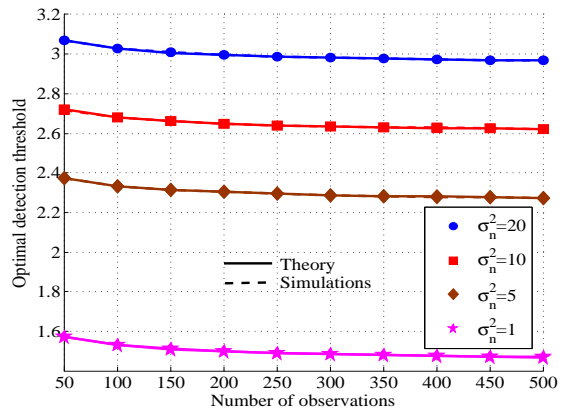


Figure 11. Optimal threshold τ_c using (A.3) and from simulations vs. M for different σ_n^2 .

under both Gaussian and bimodal mixture Gaussians, with Gaussian distributed primary and with the Rayleigh fading (vide Fig. 10) for different SNRs. We can see that DED under the bimodal Gaussian noise performs better than unimodal Gaussian counterpart. In particular, the performance of DED under bimodal Gaussian noise for -10dB SNR close to that under the unimodal Gaussian for -6dB SNR. Therefore, for a given p_d , the bimodal Gaussian model accommodates an additional 4dB decrease in SNR.

We present the behaviour of optimal detection threshold under different noise conditions, such as, Gaussian, Laplacian and mixture of Gaussians. Fig. 11 shows the optimal detection threshold of (A.3) vs. M , varying over σ_n^2 . Clearly, the simulation results are in excellent agreement with the analytically derived results. Further, the detection threshold is independent of the average primary SNR, as we employ a GoFT approach.

Next, Fig. 12 shows the agreement between the expressions derived in Appendix B and the corresponding Monte Carlo simulations. The closeness of the curves validates our claim. On the other hand, not surprisingly, comparing Fig. 11 and Fig. 12 for the same values of M and σ_n^2 clearly indicates that the detection threshold for the Laplacian case is higher for the same false alarm constraint, which is due to the fact that the Laplace distribution is heavy-tailed. This also explains the deterioration in performance for the same set of parameters under Laplacian noise which was observed earlier.

Finally, the results shown in Fig. 13 validate our analysis of Appendix C. That the analysis holds for large M and $\mu(\geq 3)$ is borne out by the fact that the disparity between the simulations and theory reduces progressively.

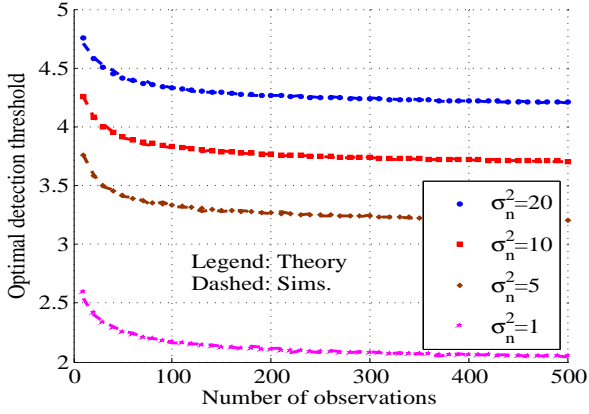


Figure 12. Optimal threshold τ_l using (B.4) and from simulations vs. M for different λ .

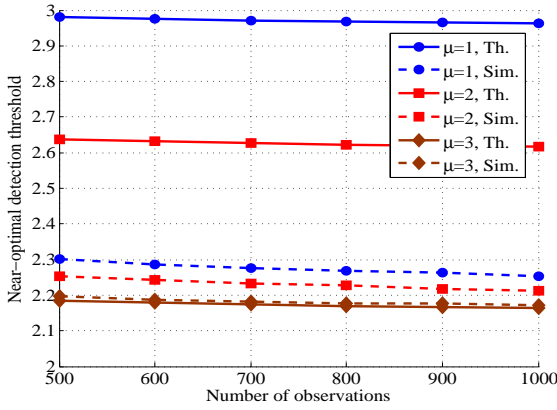


Figure 13. Near-optimal threshold τ_G^{MG} using (C.7) and from simulations vs. M and for different μ .

5. Concluding Remarks

We proposed a novel spectrum sensing technique based on differential entropy estimate with the goodness-of-fit formulation. The distribution of the test statistic under the null hypothesis and the detection threshold that satisfies a constraint on the probability of false-alarm were obtained in closed form. Through Monte Carlo simulations, it was shown that the proposed detector significantly outperforms the order statistics based detector in the low SNR regime, under various fading and primary signal models. The results with unimodal Gaussian vis-à-vis bimodal Gaussian noise process were compared. For a given probability of detection, this mixture model was shown to provide an additional leeway to the tune of 4dB in SNR over the corresponding unimodal Gaussian.

Appendix A. Calculation of τ_c

We adopt one of the many ways to arrive at the result here. Under \mathcal{H}_0 , since $Y_i \sim \mathcal{N}(0, \sigma_n^2)$, it follows from

Cochran's Theorem that the unbiased estimate, \mathcal{V} , of the variance of Y_i follows a scaled, central χ^2 distribution with $M - 1$ degrees-of-freedom. Thus,

$$\mathcal{V} \triangleq \frac{1}{M-1} \sum_{i=1}^M (Y_i - \widehat{Y})^2 \sim \frac{\sigma_n^2}{M-1} \chi_{M-1}^2,$$

which implies that the statistic $\widehat{h}(Y)$ can be written as

$$\widehat{h}(Y|\mathcal{H}_0) = \frac{1}{2} \log(2\pi e) + \frac{1}{2} \log \mathcal{V}. \quad (\text{A.1})$$

Under \mathcal{H}_0 , the statistic $\log \mathcal{V}$ follows a log-scaled, central χ^2 distribution with $M - 1$ degrees-of-freedom, represented by $\log \chi_{M-1}^2$. It is easy to show that the CDF, $F_X(\cdot)$, of the random variable $X \sim \log \chi_n^2$, is given by

$$F_X(a) \triangleq \int_{-\infty}^a f_X(x) dx = \frac{\gamma_{\text{inc}}\left(\frac{n}{2}, e^{(a-\log 2)}\right)}{\Gamma\left(\frac{n}{2}\right)},$$

where $\gamma_{\text{inc}}(\cdot, \cdot)$, and $\Gamma(\cdot)$ are the lower incomplete gamma function and the standard gamma function, respectively [14]. The proof of this result is straightforward and is omitted for brevity. Therefore, the probability of false-alarm, p_f , is given by

$$\begin{aligned} p_f &= \mathcal{P}\{\widehat{h}(Y|\mathcal{H}_0) \geq \tau_G\} \\ &= 1 - \frac{\gamma_{\text{inc}}\left(\frac{M-1}{2}, \exp\left\{2\tau_G - \log\left(\frac{4\pi e \sigma_n^2}{M-1}\right)\right\}\right)}{\Gamma\left(\frac{M-1}{2}\right)}. \end{aligned} \quad (\text{A.2})$$

Now, by simple transformations on (A.1), using (A.2), it is straightforward to show that, for $\alpha_f \in (0, 1)$, the threshold, τ_G , should be chosen to satisfy

$$1 - \frac{\gamma_{\text{inc}}\left(\frac{M-1}{2}, \exp\left\{2\tau_G - \log\left(\frac{4\pi e \sigma_n^2}{M-1}\right)\right\}\right)}{\Gamma\left(\frac{M-1}{2}\right)} = \alpha_f. \quad (\text{A.3})$$

Appendix B. Calculation of τ_l

On lines similar to those in Appendix A, for a Laplacian, it can be shown that

$$\frac{2}{\lambda} \sum_{i=1}^M |Y_i - \widehat{Y}| \sim \chi_{2M}^2.$$

Therefore, it is easily seen that

$$\widehat{h}(Y|\mathcal{H}_0) = \log_2 \left(\frac{2e}{M} \sum_{i=1}^M |Y_i - \widehat{Y}| \right)$$

follows a $\log - \chi^2$ distribution. Again, following an approach similar to that in Appendix A, it can be shown that for a given $\alpha_f \in (0, 1)$, the optimal threshold, τ_l , is required to satisfy

$$1 - \frac{\gamma_{\text{inc}}\left(M, \exp\left[\log(2) \left\{ \tau_l - \log_2\left(\frac{\lambda e}{M}\right) - 1 \right\}\right]\right)}{\Gamma(M)} = \alpha_f. \quad (\text{B.4})$$

Appendix C. Computing the Near-Optimal τ_G^{MG}

It is known that if $\{Y_i, i \in \mathcal{M}\}$ represent a set of i.i.d. random variables from any distribution, not necessarily unimodal, and with finite variance σ^2 , then the random variable defined by

$$Y_s^2 \triangleq \frac{1}{M-1} \sum_{i=1}^M (Y_i - \widehat{Y})^2,$$

has mean and variance in an asymptotic sense (as $M \rightarrow \infty$) respectively given by [15]

$$\mathbb{E}Y_s^2 = \sigma^2 \quad \text{and} \quad \text{var}(Y_s^2) = \sigma^4 \left[\frac{2}{M-1} + \frac{\kappa}{M} \right], \quad (\text{C.5})$$

where κ is the excess kurtosis and μ_4 is the fourth central moment, i.e., about the mean of the parent distribution. Therefore, for the bimodal Gaussian,

$$\begin{aligned} \mathbb{E}Y_s^2 &= \sigma_n^2 + \mu^2 \quad \text{and} \\ \text{var}(Y_s^2) &= (\sigma_n^2 + \mu^2)^2 \left[\frac{2}{M-1} + \frac{\kappa}{M} \right]. \end{aligned} \quad (\text{C.6})$$

A closed form expression for the distribution of Y_s^2 for the bimodal Gaussian distribution is hard to obtain. However, it can be well approximated in the asymptotic sense by a Gaussian distribution with moments in (C.5) and (C.6).

For large values of μ (≥ 3), $h(Y|\mathcal{H}_0)$ can be approximated as [11]

$$h(Y|\mathcal{H}_0) \approx \frac{1}{2} \log(2\pi e \sigma_n^2) + \log 2.$$

Hence, an estimate of the above entropy is given by

$$\begin{aligned} \widehat{h}(Y|\mathcal{H}_0) &= \frac{1}{2} \log \left(\frac{2\pi e}{M-1} \sum_{i=1}^M (Y_i - \widehat{Y}_i)^2 \right) + \log 2 \\ &= \frac{1}{2} \log(4\pi e Y_s^2). \end{aligned}$$

Therefore, the probability of false-alarm, p_f , becomes

$$\begin{aligned} p_f &= \mathcal{P} \left\{ \widehat{h}(Y) \geq \tau_G^{\text{MG}} | \mathcal{H}_0 \right\} \\ &\stackrel{(a)}{=} \mathcal{P} \left\{ Y_s^2 \geq \frac{\exp(2\tau_G^{\text{MG}} - 1)}{4\pi} \right\} \\ &= \mathcal{Q} \left[\frac{\exp(2\tau_G^{\text{MG}} - 1) - \mathbb{E}Y_s^2}{\sqrt{\text{var}(Y_s^2)}} \right], \end{aligned}$$

where $\stackrel{(a)}{=}$ denotes that the equality holds due to the fact that $\log(\cdot)$ is monotone, and $\mathcal{Q}(\cdot)$ denotes the Q-function. Now, it is straightforward to show that, given $\alpha_f \in (0, 1)$,

the near-optimal threshold, τ_G^{MG} , is

$$\tau_G^{\text{MG}} = 0.5 \log \left(4\pi e \left\{ (\sigma_n^2 + \mu^2) \left[\mathcal{Q}^{-1}(\alpha_f) \sqrt{\left(\frac{2}{M-1} + \frac{\kappa}{M} \right) + 1} \right] \right\} \right). \quad (\text{C.7})$$

Acknowledgement. This work was supported and funded by CMR Institute of Technology, 132, AECS Layout, ITPL Road, Bengaluru 560037, INDIA. Weblink: www.cmrit.ac.in

References

- [1] Gurugopinath, S., Muralishankar, R., Shankar, H. N.: Differential Entropy Driven Goodness-of-Fit Test For Spectrum Sensing. Proc. CROWNCOM 2015, (2015)
- [2] Wang, H., Yang, E.-H., Zhao, Z., Zhang, W.: Spectrum Sensing in Cognitive Radio Using Goodness of Fit Testing. IEEE Trans. Wireless Commun., vol. 8, no. 11, 5427-5430, (2009)
- [3] Shen, L., Wang, H., Zhang, W., Zhao, Z.: Blind Spectrum Sensing for Cognitive Radio Channels with Noise Uncertainty. IEEE Trans. Wireless Commun., vol. 10, no. 6, 1721-1724, (2011)
- [4] Rostami, S., Arshad, K., Moessner, K.: Order-Statistic Based Spectrum Sensing for Cognitive Radio. IEEE Commun. Lett., vol. 16, no. 5, 592-595, (2012)
- [5] Gurugopinath, S., Murthy, C. R., Seelamantula, C. S.: Zero Crossings Based Spectrum Sensing Under Noise Uncertainties. Proc. NCC, (2014)
- [6] Denkovski, D., Atanasovski, V., Gavrilovska, L.: HOS Based Goodness-of-Fit Testing Signal Detection. IEEE Commun. Lett., vol. 16, no. 3, 310-313, (2012)
- [7] Nguyen-Thanh, N., Kieu-Xuan, T., Koo, I.: Comments and Corrections on "Spectrum Sensing in Cognitive Radio using Goodness-of-Fit Testing". IEEE Trans. Wireless Commun., vol. 11, no. 10, 3409-3411, (2012)
- [8] Rohde, G., Nichols, J., Bucholtz, F., Michalowicz, J.: Signal Estimation Based on Mutual Information Maximization. Proc. ACSSC, 597-600, (2007)
- [9] Cover, T. M., Thomas, J. M.: Elements of Information Theory. 2nd ed. John Wiley and Sons, Inc., (2005)
- [10] Wang, Y., Wu, L.: Nonlinear Signal Detection From an Array of Threshold Devices for Non-Gaussian Noise. Digit. Signal Process., vol. 17, no. 1, 76-89, (2007)
- [11] Michalowicz, J. V., Nichols, J. M., Bucholtz, F.: Calculation of Differential Entropy for a Mixed Gaussian Distribution. Entropy, vol. 10, no. 3, 200-206, (2008)
- [12] Hashemi, H.: The Indoor Radio Propagation Channel. Proceedings of the IEEE, vol. 81, no. 7, 943-968, (1993)
- [13] Axell, E., Leus, G., Larsson, E., Poor, H. V.: Spectrum Sensing for Cognitive Radio: State-of-the-Art and Recent Advances. IEEE Signal Process. Mag., vol. 29, no. 3, 101-116, (2012)
- [14] Gradshteyn, I., Ryzhik, I.: Tables of integrals, series and products. 7th ed. Academic Press, (2007)
- [15] Mood, A. M., Graybill, F. A., Boes, D. C.: Introduction to the Theory of Statistics, 3rd ed. McGraw-Hill, (1974)